

Effects of variations of SUSY breaking scale on neutrino parameters at low energy scale under radiative corrections

Kh. Helensana Devi ^{*1}, K. Sashikanta Singh ^{†1}, and N.Nimai Singh ^{‡ 1,2}

¹Department of Physics, Manipur University, Imphal-795003, India
²Research Institute of Science and Technology, Imphal-795003, India

Abstract

The paper addresses the effects of the variations of the SUSY breaking scale m_s in the range (2-14) TeV on the three neutrino masses and mixings, in running the renormalization group equations (RGEs) for different input values of high energy seesaw scale M_R , in both normal and inverted hierarchical neutrino mass models. The present investigation is a continuation of the earlier works based on the variation of m_s scale. Two approaches are adopted one after another - bottom-up approach for running gauge and Yukawa couplings from low to high energy scale, followed by the top-down approach from high to low energy scale for running neutrino parameters defined at high energy scale, along with gauge and Yukawa couplings. A self-complementarity relation among three mixing angles is also employed in the analysis. Significant effect due to radiative corrections on neutrino parameters with the variation of SUSY breaking scale m_s , is observed.

Keywords: Self-complementarity relation, supersymmetry breaking scale, seesaw scale, RGEs, NH case, IH case, SM, MSSM.

^{*}helensanakhumanthem2@manipuruniv.ac.in

[†]ksm1skynet@gmail.com

[‡]nimai03@yahoo.com

1 Introduction

Neutrino physics has registered significant progress in recent years with the measurement of non-zero θ_{13} [1, 2, 3] and Dirac CP phase [4, 5], thus indicating a possibility for a sizable CP violation in neutrino sector. Neutrino oscillations [6, 7, 8] have been well studied with the precise measurements of neutrino mass parameters and mixing angles. But till date there are still some unsettled questions in neutrino physics such as the correct mass hierarchical order whether normal or inverted, absolute neutrino mass scale, nature of neutrino whether Dirac or Majorana type, the exact scale of seesaw mechanism, the supersymmetric breaking scale if all it exists, to mention a few. The information related to the absolute neutrino masses, has been continuously updating with the recent PLANCK data on cosmological upper bound [9, 10] on the sum of three neutrino masses $\Sigma|m_i| < 0.12$ eV, neutrinoless double beta decay [11, 12] results with the upper bound in the overall range $m_{ee} < (0.075 - 0.350)$ eV and KATRIN [13] result on direct kinematic measurement with the upper bound $m_{\nu_e} < 0.8$ eV. Neutrino mass model if any, is bound to be consistent with these upper bounds on absolute neutrino masses.

On theoretical front, the presence of supersymmetry (SUSY) [14, 15, 16] enables to ensure the stability of hierarchy between the weak and GUT scales with the possible cancellation of quadratic term in radiative corrections to the Higgs boson mass. It is needed to have a precise unification point of three gauge couplings at high GUT scale around 2×10^{16} GeV [17, 18, 19]. It can also provide a natural mechanism for understanding the electroweak symmetry breaking (EWSB) [20] and Higgs physics. Minimal Supersymmetric Standard Model (MSSM) [21] is thus a straightforward extension of the Standard Model (SM) with minimum number of new parameters. All the particles in the same supersymmetric multiplet would have the same mass if the supersymmetry is an exact symmetry. So far there is no clear evidence for the presence of supersymmetric particles in the ongoing Large Hadron Colliders (LHC) and LHC has almost reached its maximum energy of about 14 TeV [22, 23]. While the existence of supersymmetric particles has been continuously ruling out in LHC, the supersymmetric breaking scale (m_s) still remains as an unknown parameter. There are speculations that SUSY particles may have a wide spectrum and are not confined to a single energy scale. For simplicity, one can assume a single scale [24, 25] for all supersymmetric particles and this kind of assumption is valid as long as the

m_z or $m_t \ll m_s$ [26, 27]. We assume that the m_s scale may lie somewhere in between 2 TeV and 14 TeV within the scope of LHC. The effects of the variations of SUSY breaking scale on the unification of gauge couplings and also Yukawa couplings in MSSM and SUSY GUT models, have already been addressed using two-loop RGEs for gauge and Yukawa couplings within the minimal supersymmetric SU(5) model[19], while ignoring for simplicity the threshold effects of the heavy particles, which could be as large as a few percentages. It has already been reported that for gauge couplings, the unification point increases with the increase in the SUSY breaking scale, but for Yukawa couplings the unification points decrease with the increase in SUSY breaking in the reverse order compared to the gauge couplings [19]. This finding has certain implications in other important issues such as running of the renormalization group equations (RGEs) [28, 29, 30] for neutrino masses and mixings from high energy seesaw scale to low energy electroweak scale. In this direction a preliminary analysis with normal hierarchical model has already been carried out on the stability of neutrino parameters and self-complementarity relation [30] with varying SUSY breaking scale m_s .

The present investigation is a continuation of our previous work on neutrino masses and mixings with varying SUSY breaking scale in the running of RGEs [19, 30]. We shall address both normal hierarchical and inverted hierarchical neutrino mass models, in both approaches - in the first place, bottom-up approach for running gauge and Yukawa couplings from low to high energy scale, and in the second place, top-down approach for running neutrino parameters defined at high energy scale, along with gauge and Yukawa couplings, from high to low energy scale. A self-complementarity relation among three mixing angles, $\theta_{23} \approx \theta_{12} + \theta_{13}$ is also employed in the analysis.

The paper is organised as follows. In section 2 we give a brief discussion of gauge and Yukawa couplings RGEs mainly on bottom-up and top-down runnings. In section 3, we present the numerical analysis and results. Summary and discussion are presented in section 4. We give relevant RGEs for gauge, Yukawa and quartic Higgs couplings in two-loops for both the SM and MSSM in Appendix A and RGEs of neutrino parameters in Appendix B.

2 Renormalisation Group Equations (RGEs)

We study the radiative corrections to neutrino parameters using Renormalisation Group Equations (RGEs) [19, 29, 31] with and without SUSY in two different steps using the low energy observational input values, bottom-up running from low to high energy scale for gauge and Yukawa couplings, and top-down running from high to low energy scale for neutrino mass parameters and mixing angles, along with gauge and Yukawa couplings which are already evaluated at high energy scale M_R .

2.1 Bottom-up Running

In the bottom-up running of the RGEs, we divide it into three regions, $m_z < \mu < m_t$, $m_t < \mu < m_s$, $m_s < \mu < M_R$. We use recent experimental data [8, 32] as initial input values at low energy scale, given in Table 1.

Mass(GeV)	Coupling constants	Weinberg mixing angle
$m_z(m_z)= 91.1876$	$\alpha_{em}^{-1}(m_z) = 127.952 \pm 0.009$	$\sin^2 \theta_w(m_z) = 0.23121 \pm 0.00017$
$m_t(m_t)= 172.76$	$\alpha_s(m_z) = 0.1179 \pm 0.009$	
$m_b(m_b)= 4.18$		
$m_\tau(m_\tau)= 1.77$		

Table 1: Latest experimental data for fermion masses, gauge coupling constants and Weinberg mixing angle.

The values of gauge couplings, α_2 for $SU(2)_L$ and α_1 for $U(1)_Y$, are calculated by using $\sin^2 \theta_w(m_z) = \frac{\alpha_{em}(m_z)}{\alpha_2(m_z)}$ and matching condition,

$$\frac{1}{\alpha_{em}(m_z)} = \frac{5}{3} \frac{1}{\alpha_1(m_z)} + \frac{1}{\alpha_2(m_z)}. \quad (1)$$

We can also express the gauge couplings α_i 's [19] in terms of normalized couplings g_i 's as $g_i = \sqrt{4\pi\alpha_i}$, where $i = 1, 2, 3$ denote electromagnetic, weak and strong couplings respectively. RGEs at one-loop level [33] is used for evolution of the three gauge coupling constants from m_z scale to m_t scale, as given below:

$$\frac{1}{\alpha_i(\mu)} = \frac{1}{\alpha_i(m_z)} - \frac{b_i}{2\pi} \ln \frac{\mu}{m_z}, \quad (2)$$

where $m_z \leq \mu \leq m_t$ and $b_i = (5.30, -0.50, -4.00)$ for non-SUSY case. For fermion masses to define at m_t scale, we use QED-QCD rescaling factor η [34], $m_b(m_t) = \frac{m_b(m_b)}{\eta_b}$ and $m_\tau(m_t) = \frac{m_\tau(m_\tau)}{\eta_\tau}$, where $\eta_b = 1.53$ and $\eta_\tau = 1.015$. We then convert them to Yukawa couplings, $h_t(m_t) = \frac{m_t(m_t)}{v_0}$, $h_b(m_t) = \frac{m_b(m_b)}{v_0\eta_b}$, and $h_\tau(m_\tau) = \frac{m_\tau(m_\tau)}{v_0\eta_\tau}$, where $v_0 = 174$ GeV is the vacuum expectation of SM Higgs field. The calculated numerical values for fermion masses, Yukawa and gauge couplings at m_t scale are given in Table 2.

Fermions masses	Yukawa Couplings	Gauge Couplings
$m_t(m_t) = 172.76$ GeV	$h_t(m_t) = 0.9928$	$g_1(m_t) = 0.4635$
$m_b(m_t) = 2.73$ GeV	$h_b(m_t) = 0.0157$	$g_2(m_t) = 0.6511$
$m_\tau(m_t) = 1.75$ GeV	$h_\tau(m_t) = 0.0100$	$g_3(m_t) = 1.1890$

Table 2: Numerical values for fermion masses, Yukawa and gauge couplings at m_t scale.

We study the effect of variation of SUSY breaking scale (m_s) on gauge and Yukawa couplings for running from m_t to the M_R scale using RGEs which are given in Appendix A. At m_s scale, the following matching conditions are applied at the transition point from SM ($m_t < \mu < m_s$) to MSSM ($m_s < \mu < M_R$) as

$$\left. \begin{aligned} g_i(SUSY) &= g_i(SM) \\ h_t(SUSY) &= \frac{h_t(SM)}{\sin\beta} = h_t(SM) \times \frac{\sqrt{1+\tan^2\beta}}{\tan\beta} \\ h_b(SUSY) &= \frac{h_b(SM)}{\cos\beta} = h_b(SM) \times \sqrt{1+\tan^2\beta} \\ h_\tau(SUSY) &= \frac{h_\tau(SM)}{\cos\beta} = h_\tau(SM) \times \sqrt{1+\tan^2\beta} \end{aligned} \right\} \quad (3)$$

The output for Yukawa and gauge couplings at M_R scale, are given in Table 3 for $M_R = 10^{13}$ GeV, Table 4 for $M_R = 10^{14}$ GeV, Table 5 for $M_R = 10^{15}$ GeV and Table 6 for $M_R = 10^{16}$ GeV respectively, for common value of $\tan\beta = 40$. These values are needed for the next top - down running as input values at high energy scale.

$m_s(\text{TeV})$	h_t	h_b	h_τ	g_1	g_2	g_3
2	0.6509	0.3139	0.3721	0.6086	0.6914	0.7743
4	0.6318	0.3102	0.3741	0.6043	0.6861	0.7700
6	0.6236	0.3086	0.3750	0.6023	0.6835	0.7679
8	0.6161	0.3071	0.3760	0.6002	0.6810	0.7658
10	0.6126	0.3063	0.3765	0.5992	0.6797	0.7648
12	0.6093	0.3056	0.3770	0.5981	0.6785	0.7638
14	0.6061	0.3050	0.3775	0.5971	0.6772	0.7628

Table 3: Values of Yukawa and gauge couplings evaluated at $t_R = \ln(10^{13} \text{ GeV}) = 29.93$ for $\tan \beta = 40$, for different choices of m_s scale.

$m_s(\text{TeV})$	h_t	h_b	h_τ	g_1	g_2	g_3
2	0.6289	0.2977	0.3650	0.6316	0.6982	0.7554
4	0.6104	0.2946	0.3674	0.6268	0.6915	0.7514
6	0.6022	0.2931	0.3684	0.6245	0.6889	0.7495
8	0.5947	0.2917	0.3695	0.6222	0.6863	0.7475
10	0.5913	0.2910	0.3700	0.6211	0.6850	0.7466
12	0.5879	0.2904	0.3705	0.6199	0.6837	0.7456
14	0.5848	0.2898	0.3710	0.6188	0.6824	0.7447

Table 4: Values of Yukawa and gauge couplings evaluated at $t_R = \ln(10^{14} \text{ GeV}) = 32.23$ for $\tan \beta = 40$, for different choices of m_s scale.

$m_s(\text{TeV})$	h_t	h_b	h_τ	g_1	g_2	g_3
2	0.6084	0.2829	0.3579	0.6574	0.7026	0.7378
4	0.5891	0.2798	0.3601	0.6521	0.6971	0.7341
6	0.5809	0.2784	0.3613	0.6494	0.6944	0.7323
8	0.5735	0.2771	0.3624	0.6468	0.6917	0.7305
10	0.5701	0.2766	0.3629	0.6455	0.6903	0.7296
12	0.5668	0.2760	0.3635	0.6443	0.6890	0.7287
14	0.5637	0.2754	0.3640	0.6430	0.6877	0.7278

Table 5: Values of Yukawa and gauge couplings $t_R = \ln(10^{15} \text{ GeV}) = 34.53$ for $\tan \beta = 40$, for different choices of m_s scale.

$m_s(\text{TeV})$	h_t	h_b	h_τ	g_1	g_2	g_3
2	0.5854	0.2676	0.3494	0.6893	0.7089	0.7200
4	0.5661	0.2647	0.3518	0.6831	0.7032	0.7166
6	0.5580	0.2634	0.3529	0.6801	0.7004	0.7149
8	0.5680	0.2687	0.3622	0.6770	0.6664	0.7131
10	0.5473	0.2618	0.3547	0.6757	0.6963	0.7124
12	0.5441	0.2613	0.3553	0.6742	0.6949	0.7116
14	0.5410	0.2608	0.3559	0.6727	0.6936	0.7107

Table 6: Values of Yukawa and gauge couplings evaluated at $t_R = \ln(10^{16} \text{ GeV}) = 36.84$ for $\tan \beta = 40$, for different choices of m_s scale.

2.2 Top-down Running

In this running, we use the values of Yukawa and gauge couplings which are found at M_R scale as initial inputs. We give the sum of three neutrino masses in the range, $\Sigma|m_i| \approx 0.11 \text{ eV}$ for NH case and $\Sigma|m_i| \approx 0.10 \text{ eV}$ for IH case. Using all the necessary mathematical frameworks, we analyze the radiative nature of neutrino parameters like neutrino masses, mixings, CP phases, using top-down approach with the variations of m_s scale at different M_R scale, using respective RGEs which are given in Appendix B. The input sets are given in Table 7 and Table 8.

Input parameters	Seesaw scale ($\tan \beta = 40^0$)			
	10^{16} GeV	10^{15} GeV	10^{14} GeV	10^{13} GeV
$m_1(\text{eV})$	0.0262	0.0258	0.0271	0.0274
$m_2(\text{eV})$	-0.0263	-0.0259	-0.0272	-0.0275
$m_3(\text{eV})$	-0.0615	-0.0645	-0.0643	-0.0664
$ \Sigma m_i $	0.114	0.116	0.118	0.121
$\theta_{12}/^0$	32.46	33.95	33.01	32.61
$\theta_{13}/^0$	7.39	7.56	7.64	7.70
$\psi/^0$	180	180	180	180
$\delta/^0$	240	240	240	240

Table 7: Input set of neutrino parameters at high energy scale M_R for NH case. θ_{23} is used from SC relation, $\theta_{23} = q \times (\theta_{13} + \theta_{12})$ with $q=1.1$. This is common for all cases of m_s scale.

Input parameters	Seesaw scale ($\tan \beta = 40^0$)			
	10^{16} GeV	10^{15} GeV	10^{14} GeV	10^{13} GeV
m_1 (eV)	0.0515	0.0501	0.0511	0.0523
m_2 (eV)	-0.0516	-0.0502	-0.0512	-0.0524
m_3 (eV)	-0.0025	-0.0021	-0.0022	-0.0025
$ \Sigma m_i $	0.1056	0.1024	0.1045	0.1072
$\theta_{12}/^0$	31.94	32.39	31.99	32.17
$\theta_{13}/^0$	8.53	8.29	8.35	8.40
$\psi/^0$	180	180	180	180
$\delta/^0$	240	240	240	240

Table 8: Input set of neutrino parameters at high energy scale M_R for IH case ($m_3 \neq 0$). θ_{23} is used from SC relation, $\theta_{23} = q \times (\theta_{13} + \theta_{12})$ with $q=1.1$. This is common for all cases of m_s scale.

3 Numerical Analysis and Results

The effects of the variation of m_s on the outputs of neutrino mass parameters and mixing angles are given in Tables 9 - 12, along with the graphical representations in Figures 2 for normal hierarchical (NH) model; and in Tables 13 - 16 and Figures 1 for inverted hierarchical (IH) case. In each case we also present the results for variation of high energy seesaw scale (10^{13} - 10^{16}) GeV. Similar patterns with the variations of seesaw scale are observed in all the Figures 1 and 2.

m_s scale (TeV)	Δm_{31}^2 ($10^{-3} eV^2$)	Δm_{21}^2 ($10^{-5} eV^2$)	θ_{23} (0)	θ_{12} (0)	θ_{13} (0)	δ (0)	$ \Sigma m_i $ (eV)
2	2.504	4.831	45.37	32.69	8.40	235.26	0.095
4	2.569	5.961	45.42	32.72	8.47	235.36	0.094
6	2.593	6.666	45.45	32.73	8.52	235.41	0.094
8	2.614	6.962	45.47	32.74	8.54	235.43	0.094
10	2.621	7.288	45.48	32.75	8.56	235.45	0.093
12	2.624	7.526	45.50	32.75	8.58	235.47	0.093
14	2.620	7.779	45.52	32.76	8.60	235.49	0.092

Table 9: Effects on the output of neutrino parameters at low energy scale, on varying m_s for NH case ($\tan \beta = 40$, $M_R \sim 10^{13}$ GeV).

m_s scale (TeV)	Δm_{31}^2 ($10^{-3}eV^2$)	Δm_{21}^2 ($10^{-5}eV^2$)	θ_{23} ($^\circ$)	θ_{12} ($^\circ$)	θ_{13} ($^\circ$)	δ ($^\circ$)	$ \Sigma m_i $ (eV)
2	2.336	4.771	45.75	32.09	8.35	235.08	0.092
4	2.418	5.850	45.79	32.11	8.41	235.16	0.093
6	2.428	6.541	45.82	33.13	8.46	235.22	0.092
8	2.435	6.859	45.84	33.14	8.48	235.24	0.091
10	2.440	7.180	45.86	33.15	8.51	235.27	0.091
12	2.441	7.490	45.88	33.16	8.53	235.29	0.090
14	2.454	7.654	45.89	33.16	8.55	235.30	0.090

Table 10: Effects on the output of neutrino parameters at low energy scale, on varying m_s for NH case ($\tan\beta = 40$, $M_R \sim 10^{14}$ GeV).

m_s scale (TeV)	Δm_{31}^2 ($10^{-3}eV^2$)	Δm_{21}^2 ($10^{-5}eV^2$)	θ_{23} ($^\circ$)	θ_{12} ($^\circ$)	θ_{13} ($^\circ$)	δ ($^\circ$)	$ \Sigma m_i $ (eV)
2	2.373	4.371	46.71	34.03	8.24	235.35	0.090
4	2.461	5.350	46.76	34.05	8.31	235.43	0.090
6	2.479	5.964	46.79	34.07	8.35	235.48	0.090
8	2.492	6.264	46.81	34.08	8.38	235.51	0.090
10	2.498	6.633	46.83	34.09	8.41	235.54	0.089
12	2.498	6.832	46.84	34.09	8.43	235.56	0.089
14	2.499	7.028	46.86	34.10	8.45	235.57	0.088

Table 11: Effects on the output of neutrino parameters at low energy scale, on varying m_s for NH case ($\tan\beta = 40$, $M_R \sim 10^{15}$ GeV).

m_s scale (TeV)	Δm_{31}^2 ($10^{-3}eV^2$)	Δm_{21}^2 ($10^{-5}eV^2$)	θ_{23} ($^\circ$)	θ_{12} ($^\circ$)	θ_{13} ($^\circ$)	δ ($^\circ$)	$ \Sigma m_i $ (eV)
2	2.354	4.435	44.83	32.54	8.08	234.98	0.093
4	2.427	5.459	44.87	32.56	8.14	235.07	0.094
6	2.444	6.108	44.89	32.57	8.18	235.13	0.094
8	2.472	6.457	44.91	32.58	8.20	235.16	0.094
10	2.476	6.734	44.92	32.59	8.22	235.18	0.093
12	2.475	7.033	44.94	32.60	8.24	235.21	0.093
14	2.486	7.182	44.95	32.60	8.26	235.22	0.093

Table 12: Effects on the output of neutrino parameters at low energy scale, on varying m_s for NH case ($\tan\beta = 40$, $M_R \sim 10^{16}$ GeV).

m_s scale (TeV)	$ \Delta m_{31}^2 $ ($10^{-3}eV^2$)	Δm_{21}^2 ($10^{-5}eV^2$)	θ_{23} ($^\circ$)	θ_{12} ($^\circ$)	θ_{13} ($^\circ$)	δ ($^\circ$)	$ \Sigma m_i $ (eV)
2	2.58	5.96	44.70	32.21	8.41	239.94	0.119
4	2.55	6.64	44.71	32.22	8.41	239.93	0.117
6	2.53	7.10	44.72	32.22	8.41	239.93	0.116
8	2.52	7.32	44.73	32.23	8.41	239.92	0.115
10	2.52	7.52	44.73	32.23	8.41	239.92	0.114
12	2.51	7.73	44.74	32.23	8.41	239.92	0.114
14	2.50	7.86	44.74	32.23	8.41	239.92	0.113

Table 13: Effects on the output of neutrino parameters at low energy scale, on varying m_s for IH case ($\tan \beta = 40$, $M_R \sim 10^{13}$ GeV).

m_s scale (TeV)	$ \Delta m_{31}^2 $ ($10^{-3}eV^2$)	Δm_{21}^2 ($10^{-5}eV^2$)	θ_{23} ($^\circ$)	θ_{12} ($^\circ$)	θ_{13} ($^\circ$)	δ ($^\circ$)	$ \Sigma m_i $ (eV)
2	2.46	5.68	44.44	32.04	8.35	239.95	0.114
4	2.44	6.30	44.46	32.05	8.35	239.94	0.112
6	2.42	6.75	44.47	32.05	8.35	239.93	0.110
8	2.41	7.05	44.48	32.05	8.35	239.93	0.106
10	2.40	7.25	44.48	32.06	8.35	239.93	0.109
12	2.40	7.37	44.49	32.06	8.35	239.93	0.108
14	2.39	7.49	44.49	32.06	8.35	239.92	0.108

Table 14: Effects on the output of neutrino parameters at low energy scale, on varying m_s for IH case ($\tan \beta = 40$, $M_R \sim 10^{14}$ GeV).

m_s scale (TeV)	$ \Delta m_{31}^2 $ ($10^{-3}eV^2$)	Δm_{21}^2 ($10^{-5}eV^2$)	θ_{23} ($^\circ$)	θ_{12} ($^\circ$)	θ_{13} ($^\circ$)	δ ($^\circ$)	$ \Sigma m_i $ (eV)
2	2.37	5.56	44.82	32.44	8.29	239.95	0.111
4	2.34	6.11	44.84	32.45	8.29	239.94	0.109
6	2.33	6.55	44.85	32.45	8.29	239.94	0.107
8	2.32	6.73	44.85	32.45	8.29	239.93	0.107
10	2.31	6.91	44.86	32.46	8.29	239.93	0.106
12	2.30	7.15	44.87	32.46	8.29	239.93	0.105
14	2.30	7.23	44.87	32.46	8.29	239.93	0.105

Table 15: Effects on the output of neutrino parameters at low energy scale, on varying m_s for IH case ($\tan \beta = 40$, $M_R \sim 10^{15}$ GeV).

m_s scale (TeV)	$ \Delta m_{31}^2 $ ($10^{-3}eV^2$)	Δm_{21}^2 ($10^{-5}eV^2$)	θ_{23} ($^\circ$)	θ_{12} ($^\circ$)	θ_{13} ($^\circ$)	δ ($^\circ$)	$ \Sigma m_i $ (eV)
2	2.51	5.22	44.59	31.98	8.54	239.94	0.118
4	2.49	5.73	44.60	31.98	8.54	239.93	0.116
6	2.47	6.14	44.61	31.99	8.54	239.93	0.115
8	2.47	6.26	44.62	31.99	8.54	239.92	0.114
10	2.46	6.46	44.62	31.99	8.54	239.92	0.114
12	2.45	6.68	44.63	32.00	8.54	239.92	0.113
14	2.45	6.74	44.63	32.00	8.54	239.92	0.112

Table 16: Effects on the output of neutrino parameters at low energy scale, on varying m_s for IH case ($\tan\beta = 40$, $M_R \sim 10^{16}$ GeV). Four different choices of M_R scale are presented.

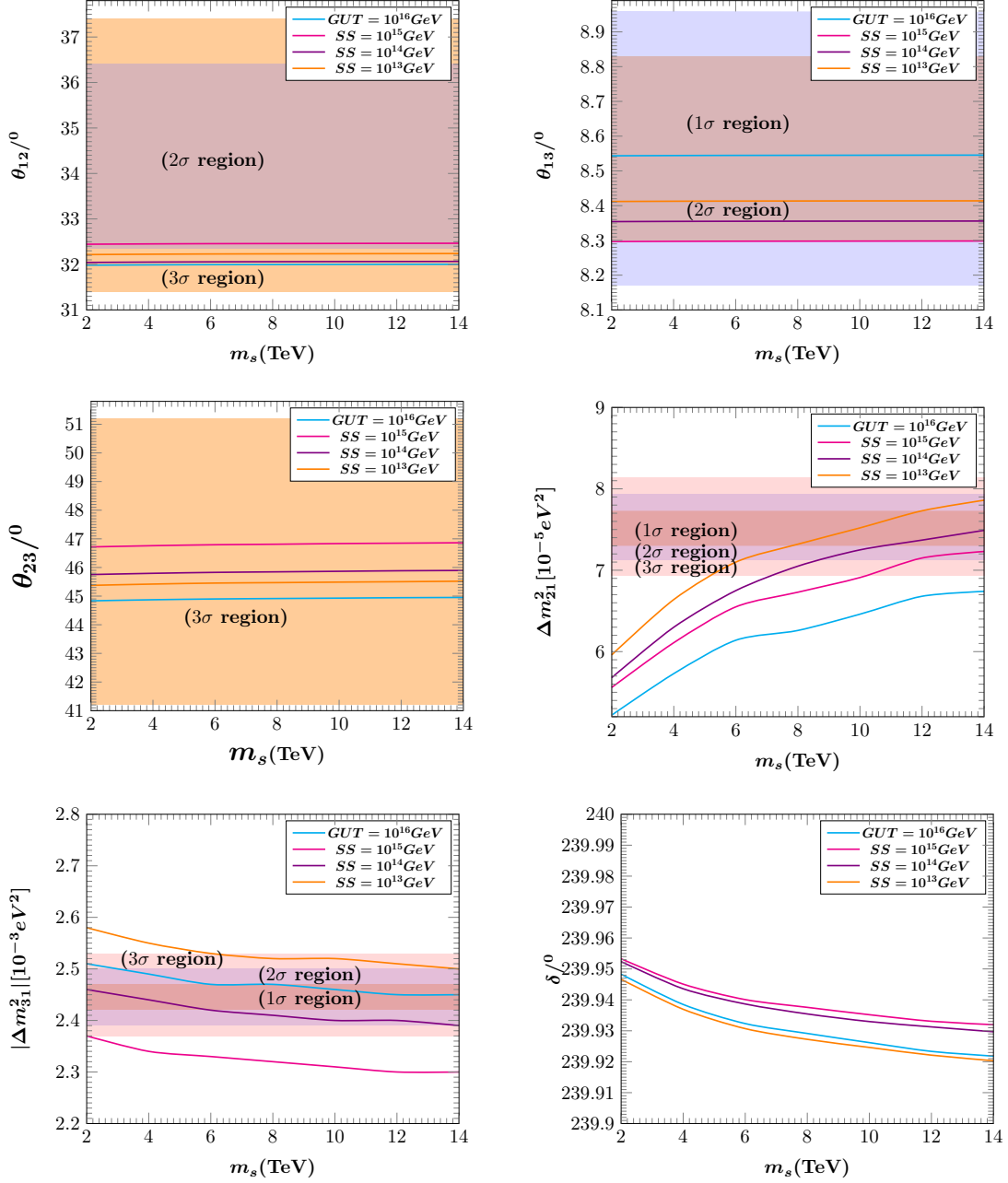


Figure 1: Effects on the low energy output results in θ_{ij} , $|\Delta m_{ij}^2|$ and δ with variation of m_s for IH (QD) case at $\tan\beta = 40$. Four different choices of M_R scale are presented.

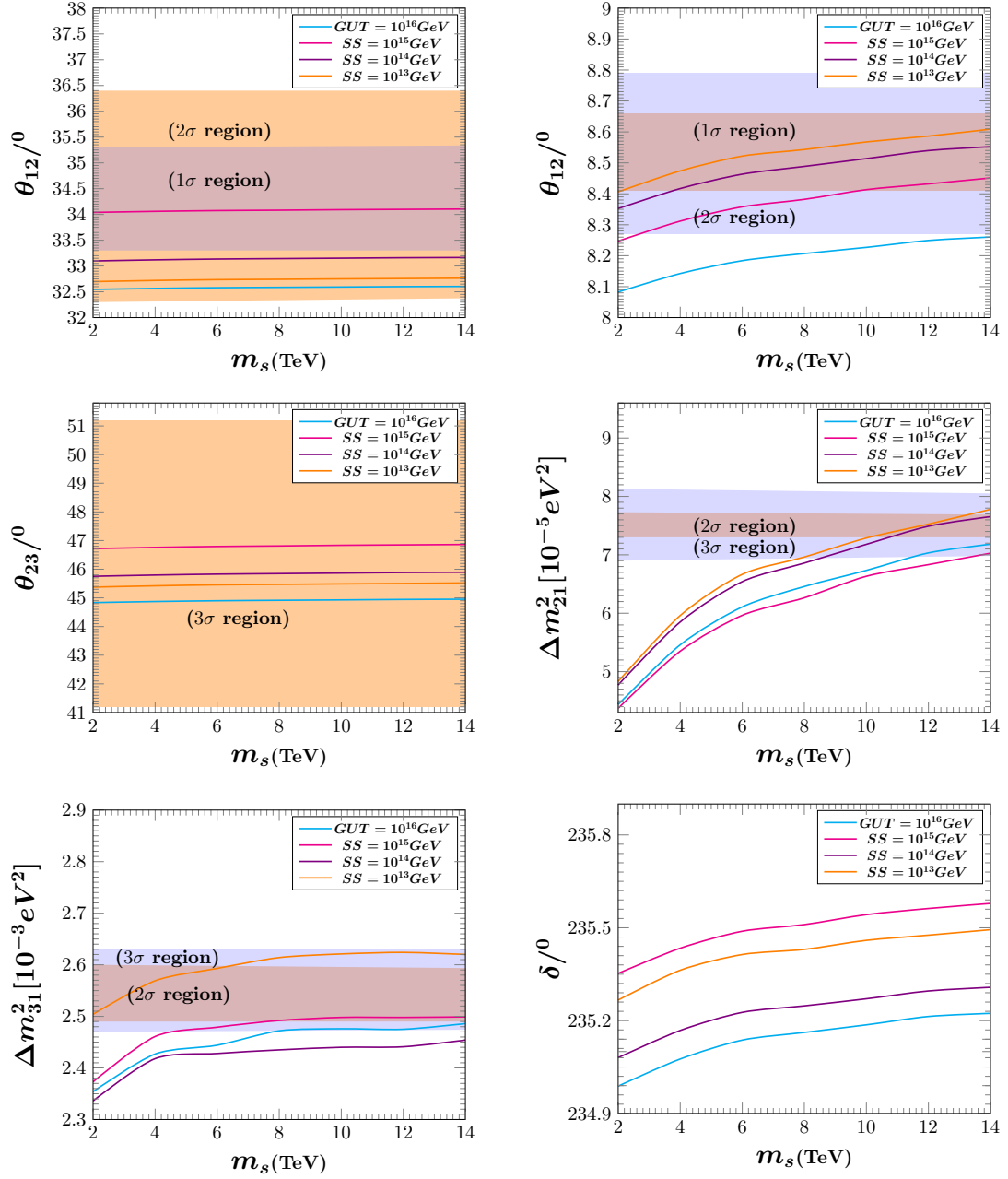


Figure 2: Effects on the low energy output results in θ_{ij} , $|\Delta m_{ij}^2|$ and δ with variation of m_s for NH(QD) case at $\tan\beta = 40$. Four different choices of M_R scale are presented.

4 Summary and Discussion

To summarize, as a continuation of the earlier investigations [19] we have studied the running of the RGEs from high scale to low scale and possible effects of the variations of SUSY breaking scale m_s in the range (2-14) TeV on two neutrino mass parameters and three mixing angles, including phases, in both normal [30] and inverted hierarchical neutrino mass models. Though $\tan\beta$ is arbitrary, we consider a fixed value of $\tan\beta = 40$ for simplicity in both cases. Effects on the variation of seesaw scale in the range ($10^{13} - 10^{16}$) GeV along with the variation of m_s , is also studied numerically. Significant effects have been observed for the increase of mass parameters and mixing angles with the increase of SUSY breaking scale in NH case, but decreases with m_s scale for IH case. The corresponding changes in CP phases are insensitive on variation of m_s scale. The analysis is consistent with the latest cosmological bound on the sum of three neutrino masses.

The present analysis can be applied to check the validity of certain mixing patterns such as Tribimaximal and Golden ratio mixing patterns at high energy scale [35, 36].

APPENDIX A

RGEs for gauge couplings [31]:

The two loop RGEs for gauge couplings are given by

$$\frac{dg_i}{dt} = \frac{b_i}{16\pi^2}g_i^3 + \frac{1}{(16\pi^2)^2} \left[\sum_{j=1}^3 b_{ij}g_i^3g_j^2 - \sum_{j=t,b,\tau} a_{ij}g_i^3h_j^2 \right], \quad (4)$$

where $t = \ln \mu$ and b_i, b_{ij}, a_{ij} are β function coefficients in MSSM,

$$b_i = (6.6, \quad 1.0, \quad -3.0), \quad b_{ij} = \begin{pmatrix} 7.96 & 5.40 & 17.60 \\ 1.80 & 25.00 & 24.00 \\ 2.20 & 9.00 & 14.00 \end{pmatrix},$$

$$a_{ij} = \begin{pmatrix} 5.2 & 2.8 & 3.6 \\ 6.0 & 6.0 & 2.0 \\ 4.0 & 4.0 & 0.0 \end{pmatrix}$$

and, for non-supersymmetric case, we have

$$b_i = (4.100, \quad -3.167, \quad -7.00), g_{ij} = \begin{pmatrix} 3.98 & 2.70 & 8.8 \\ 0.90 & 5.83 & 12.0 \\ 1.10 & 4.50 & -26.0 \end{pmatrix},$$

and

$$a_{ij} = \begin{pmatrix} 0.85 & 0.5 & 0.5 \\ 1.50 & 1.5 & 0.5 \\ 2.00 & 2.0 & 0.0 \end{pmatrix}.$$

Two-loop RGEs for Yukawa couplings and quartic Higgs coupling [31]:

For MSSM,

$$\begin{aligned} \frac{dh_t}{dt} &= \frac{h_t}{16\pi^2} \left(6h_t^2 + h_b^2 - \sum_{i=1}^3 c_i g_i^2 \right) + \frac{h_t}{(16\pi^2)^2} \left[\sum_{i=1}^3 \left(c_i b_i + \frac{c_i^2}{2} \right) g_i^4 + g_1^2 g_2^2 \right. \\ &\quad \left. + \frac{136}{45} g_1^2 g_3^2 + 8g_2^2 g_3^2 + \left(\frac{6}{5} g_1^2 + 6g_2^2 + 16g_3^2 \right) h_t^2 + \frac{2}{5} g_1^2 h_b^2 - 22h_t^4 \right. \\ &\quad \left. - 5h_b^4 - 5h_t^2 h_b^2 - h_b^2 h_\tau^2 \right], \end{aligned} \quad (5)$$

$$\begin{aligned} \frac{dh_b}{dt} &= \frac{h_b}{16\pi^2} \left(6h_b^2 + h_\tau^2 + h_t^2 - \sum_{i=1}^3 c'_i g_i^2 \right) + \frac{h_b}{(16\pi^2)^2} \left[\sum_{i=1}^3 \left(c'_i b_i + \frac{c_i'^2}{2} \right) g_i^4 \right. \\ &\quad \left. + g_1^2 g_2^2 + \frac{8}{9} g_1^2 g_3^2 + 8g_2^2 g_3^2 + \left(\frac{2}{5} g_1^2 + 6g_2^2 + 16g_3^2 \right) h_b^2 + \frac{4}{5} g_1^2 h_t^2 + \frac{6}{5} g_1^2 h_\tau^2 \right. \\ &\quad \left. - 22h_b^4 - 3h_\tau^4 - 5h_t^4 - 5h_b^2 h_t^2 - 3h_b^2 h_\tau^2 \right], \end{aligned} \quad (6)$$

$$\begin{aligned}
\frac{dh_\tau}{dt} &= \frac{h_\tau}{16\pi^2} \left(4h_\tau^2 + 3h_b^2 - \sum_{i=1}^3 c_i'' g_i^2 \right) + \frac{h_\tau}{(16\pi^2)^2} \left[\sum_{i=1}^3 \left(c_i'' b_i + \frac{c_i'''^2}{2} \right) g_i^4 \right. \\
&\quad + \frac{9}{5} g_1^2 g_2^2 + \left(\frac{6}{5} g_1^2 + 6g_2^2 \right) h_\tau^2 + \left(\frac{-2}{5} g_1^2 + 16g_3^2 \right) h_b^2 + 9g_b^4 \\
&\quad \left. - 10h_\tau^4 - 3h_b^2 h_t^2 - 9h_b^2 h_\tau^2 \right], \tag{7}
\end{aligned}$$

where

$$c_i = \left(\frac{13}{15}, \quad 3, \quad \frac{16}{13} \right), c_i' = \left(\frac{7}{15}, \quad 3, \quad \frac{16}{3} \right)$$

and

$$c_i'' = \left(\frac{9}{5}, \quad 3, \quad 0 \right).$$

For non-supersymmetric case,

$$\begin{aligned}
\frac{dh_t}{dt} &= \frac{h_t}{16\pi^2} \left(\frac{3}{2} h_t^2 - \frac{3}{2} h_b^2 + Y_2(S) - \sum_{i=1}^3 c_i g_i^2 \right) + \frac{h_t}{(16\pi^2)^2} \left[\left(\frac{1187}{600} \right) g_i^4 - \frac{23}{4} g_2^4 \right. \\
&\quad - 108g_3^4 - \frac{9}{20} g_1^2 g_2^2 + \frac{19}{15} g_1^2 g_3^2 + 9g_3^2 g_2^2 + \left(\frac{223}{80} g_1^2 + \frac{135}{16} g_2^2 + 16g_3^2 \right) h_t^2 \\
&\quad - \left(\frac{43}{80} g_1^2 - \frac{9}{16} g_2^2 + 16g_3^2 \right) h_b^2 + \frac{5}{2} Y_4(S) - 2\lambda \left(3h_t^2 + h_b^2 \right) + \frac{3}{2} h_t^4 - \frac{5}{4} h_t^2 h_b^2 \\
&\quad \left. + \frac{11}{4} h_b^4 + Y_2(S) \left(\frac{5}{4} h_b^2 - \frac{9}{4} h_t^2 \right) - \eta_4(S) + \frac{3}{2} \lambda^2 \right], \tag{8}
\end{aligned}$$

$$\begin{aligned}
\frac{dh_b}{dt} &= \frac{h_b}{16\pi^2} \left(\frac{3}{2} h_b^2 - \frac{3}{2} h_t^2 + Y_2(S) - \sum_{i=1}^3 c_i' g_i^2 \right) + \frac{h_b}{(16\pi^2)^2} \left[-\frac{127}{600} g_1^4 - \frac{23}{4} g_2^4 - 108g_3^4 \right. \\
&\quad - \frac{27}{20} g_1^2 g_2^2 + \frac{31}{15} g_1^2 g_3^2 + 9g_3^2 g_2^2 - \left(\frac{79}{80} g_1^2 - \frac{9}{16} g_2^2 + 16g_3^2 \right) h_t^2 + \left(\frac{187}{80} g_1^2 + \frac{135}{16} g_2^2 \right. \\
&\quad \left. + 16g_3^2 \right) h_b^2 + \frac{5}{2} Y_4(S) - 2\lambda \left(3h_t^2 + 3h_b^2 \right) + \frac{3}{2} h_b^4 - \frac{5}{4} h_t^2 h_b^2 + \frac{11}{4} h_t^4 \\
&\quad \left. + Y_2(S) \left(\frac{5}{4} h_t^2 - \frac{9}{4} h_b^2 \right) - \eta_4(S) + \frac{3}{2} \lambda^2 \right], \tag{9}
\end{aligned}$$

$$\begin{aligned}
\frac{dh_\tau}{dt} = & \frac{h_\tau}{16\pi^2} \left(\frac{3}{2}h_\tau^2 + Y_2(S) - \sum_{i=1}^3 c_i'' g_i^2 \right) + \frac{h_\tau}{(16\pi^2)^2} \left[\frac{1371}{200}g_1^4 - \frac{23}{4}g_2^4 - \frac{27}{20}g_1^2g_2^2 \right. \\
& + \left(\frac{387}{80}g_1^2 + \frac{135}{16}g_2^2 \right) h_\tau^2 + \frac{5}{2}Y_4(S) - 6\lambda h_t^2 + \frac{3}{2}h_\tau^4 - \frac{9}{4}Y_2(S)h_\tau^2 \\
& \left. - \eta_4(S) + \frac{3}{2}\lambda^2 \right], \tag{10}
\end{aligned}$$

$$\begin{aligned}
\frac{d\lambda}{dt} = & \frac{1}{16\pi^2} \left[\frac{9}{4} \left(\frac{3}{25}g_1^4 + \frac{2}{5}g_2^2g_1^2 + g_2^4 \right) - \left(\frac{9}{5}g_1^2 + 9g_2^2 \right) \lambda + 4Y_2(S)\lambda - 4H(S) + 12\lambda^2 \right] \\
& + \frac{1}{(16\pi^2)^2} \left[-78\lambda^3 + 18 \left(\frac{3}{5}g_1^2 + 3g_2^2 \right) \lambda^2 + \left(-\frac{73}{8}g_2^4 + \frac{117}{20}g_1^2g_2^2 + \frac{1887}{200}g_1^4 \right) \lambda \right. \\
& + \frac{305}{8}g_2^6 - \frac{867}{120}g_1^2g_2^4 - \frac{1677}{200}g_1^4g_2^2 - \frac{3411}{1000}g_1^6 - 64g_3^2 \left(h_t^4 + h_b^4 \right) - \frac{8}{5}g_1^2 \left(2h_t^4 - h_b^4 \right. \\
& \left. + 3h_\tau^4 \right) - \frac{3}{2}g_2^4Y_2(S) + 10\lambda Y_4(S) + \frac{3}{5}g_1^2 \left(-\frac{57}{10}g_1^2 + 21g_2^2 \right) h_t^2 + \left(\frac{3}{2}g_1^2 + 9g_2^2 \right) h_b^2 \\
& + \left(-\frac{15}{2}g_1^2 + 11g_2^2 \right) h_\tau^2 - 24\lambda^2Y_2(S) - \lambda H(S) + 6\lambda h_t^2 h_b^2 + 20 \left(3h_t^6 + 3h_b^6 + h_\tau^6 \right) \\
& \left. - 12 \left(h_t^4 h_b^2 + h_t^2 h_b^4 \right) \right], \tag{11}
\end{aligned}$$

where

$$\begin{aligned}
Y_2(S) &= 3h_t^2 + 3h_b^2 + h_\tau^2, \\
Y_4(S) &= \frac{1}{3} \left[3\sum c_i g_i^2 h_t^2 + 3\sum c_i' g_i^2 h_b^2 + 3\sum c_i'' g_i^2 h_\tau^2 \right],
\end{aligned}$$

$$H(S) = 3h_t^4 + 3h_b^4 + h_\tau^4,$$

$$\eta_4(S) = \frac{9}{4} \left[3h_t^4 + 3h_b^4 + h_\tau^4 - \frac{2}{3}h_t^2 h_b^2 \right]$$

and $\lambda = \frac{m_h^2}{v_0^2}$ is the Higgs self-coupling, $m_h = 125.78 \pm 0.26$ GeV is the Higgs mass [37] and $v_0 = 174$ GeV is the vacuum expectation value.

The beta function coefficients for non-SUSY case are given below:

$$c_i = (0.85, 2.25, 8.00), c_i' = (0.25, 2.25, 8.00) \text{ and } c_i'' = (2.25, 2.25, 0.00).$$

APPENDIX B

RGEs for three neutrino mixing angles and phases [28]:(neglecting higher order of θ_{13})

$$\dot{\theta}_{12} = -\frac{Cy_\tau^2}{32\pi^2} \sin 2\theta_{12} s_{23}^2 \frac{|m_1 e^{i\psi_1} + m_2 e^{i\psi_2}|^2}{\Delta m_{21}^2}, \quad (12)$$

$$\begin{aligned} \dot{\theta}_{13} &= \frac{Cy_\tau^2}{32\pi^2} \sin 2\theta_{12} \sin 2\theta_{23} \frac{m_3}{\Delta m_{31}^2 (1 + \xi)} \\ &\times \left[m_1 \cos(\psi_1 - \delta) - (1 + \xi)m_2 \cos(\psi_2 - \delta) - \xi m_3 \cos \delta \right], \quad (13) \end{aligned}$$

$$\dot{\theta}_{23} = -\frac{Cy_\tau^2}{32\pi^2} \sin 2\theta_{23} \frac{1}{\Delta m_{31}^2} \left[c_{12}^2 |m_2 e^{i\psi_2} + m_3|^2 + s_{12}^2 \frac{|m_1 e^{i\psi_1} + m_3|^2}{1 + \xi} \right], \quad (14)$$

where $\Delta m_{21}^2 = m_2^2 - m_1^2$, $\Delta m_{31}^2 = m_3^2 - m_1^2$ and $\xi = \frac{\Delta m_{21}^2}{\Delta m_{31}^2}$.

RGEs for the three phases [28]:

For dirac phase δ :

$$\dot{\delta} = \frac{Cy_\tau^2}{32\pi^2} \frac{\delta^{(-1)}}{\theta_{13}} + \frac{Cy_\tau^2}{8\pi^2} \delta^{(0)}, \quad (15)$$

where

$$\begin{aligned} \delta^{(-1)} &= \sin 2\theta_{12} \sin 2\theta_{23} \frac{m_3}{\Delta m_{31}^2 (1 + \xi)} \times \left[m_1 \sin(\psi_1 - \delta) \right. \\ &\quad \left. - (1 + \xi)m_2 \sin(\psi_2 - \delta) + \xi m_3 \sin \delta \right], \quad (16) \end{aligned}$$

$$\begin{aligned} \delta^{(0)} &= \frac{m_1 m_2 s_{23}^2 \sin(\psi_1 - \psi_2)}{\Delta m_{21}^2} \\ &+ m_3 s_{12}^2 \left[\frac{m_1 \cos 2\theta_{23} \sin \psi_1}{\Delta m_{31}^2 (1 + \xi)} + \frac{m_2 c_{23}^2 \sin(2\delta - \psi_2)}{\Delta m_{31}^2} \right] \\ &+ m_3 c_{12}^2 \left[\frac{m_1 c_{23}^2 \sin(2\delta - \psi_1)}{\Delta m_{31}^2 (1 + \xi)} + \frac{m_2 \cos(2\theta_{23}) \sin \psi_2}{\Delta m_{31}^2} \right]. \quad (17) \end{aligned}$$

For Majorana phase ψ_1 [28]:

$$\begin{aligned} \dot{\psi}_1 = & \frac{Cy_\tau^2}{8\pi^2} \left[m_3 \cos 2\theta_{23} \frac{m_1 s_{12}^2 \sin \psi_1 + (1 + \xi) m_2 c_{12}^2 \sin \psi_2}{\Delta m_{31}^2 (1 + \xi)} \right] \\ & + \frac{Cy_\tau^2}{8\pi^2} \left[\frac{m_1 m_2 c_{12}^2 s_{23}^2 \sin(\psi_1 - \psi_2)}{\Delta m_{21}^2} \right] \end{aligned} \quad (18)$$

For Majorana phase ψ_2 :

$$\begin{aligned} \dot{\psi}_2 = & \frac{Cy_\tau^2}{8\pi^2} \left[m_3 \cos 2\theta_{23} \frac{m_1 s_{12}^2 \sin \psi_1 + (1 + \xi) m_2 c_{12}^2 \sin \psi_2}{\Delta m_{31}^2 (1 + \xi)} \right] \\ & + \frac{Cy_\tau^2}{8\pi^2} \left[\frac{m_1 m_2 s_{12}^2 s_{23}^2 \sin(\psi_1 - \psi_2)}{\Delta m_{21}^2} \right] \end{aligned} \quad (19)$$

RGEs for neutrino mass eigenvalues [28]:

$$\dot{m}_1 = \frac{1}{16\pi^2} [\alpha + Cy_\tau^2 (2s_{12}^2 s_{23}^2 + F_1)] m_1, \quad (20)$$

$$\dot{m}_2 = \frac{1}{16\pi^2} [\alpha + Cy_\tau^2 (2c_{12}^2 s_{23}^2 + F_2)] m_2, \quad (21)$$

$$\dot{m}_3 = \frac{1}{16\pi^2} [\alpha + 2Cy_\tau^2 c_{13}^2 c_{23}] m_3, \quad (22)$$

where

$$F_1 = -s_{13} \sin 2\theta_{12} \sin 2\theta_{23} \cos \delta + 2s_{13}^2 c_{12}^2 c_{23}^2, \quad (23)$$

$$F_2 = s_{13} \sin 2\theta_{12} \sin 2\theta_{23} \cos \delta + 2s_{13}^2 s_{12}^2 s_{23}^2. \quad (24)$$

For MSSM case:

$$\alpha = -\frac{6}{5}g_1^2 - 6g_2^2 + 6y_t^2$$

and

$$C = 1.$$

For SM case:

$$\alpha = -3g_2^2 + 2y_\tau^2 + 6y_t^2 + 6y_b^2 + \lambda,$$

$$C = -\frac{3}{2}$$

and λ is the Higgs self-coupling in the SM.

Acknowledgements

One of the author (KHD) would like to thank Manipur University for financial support.

References

- [1] D. Adey *et al.*, “Measurement of the Electron Antineutrino Oscillation with 1958 Days of Operation at Daya Bay,” *Phys. Rev. Lett.*, vol. 121, no. 24, p. 241805, 2018.
- [2] Y. Abe *et al.*, “Indication of Reactor $\bar{\nu}_e$ Disappearance in the Double Chooz Experiment,” *Phys. Rev. Lett.*, vol. 108, p. 131801, 2012.
- [3] G. Bak *et al.*, “Measurement of Reactor Antineutrino Oscillation Amplitude and Frequency at RENO,” *Phys. Rev. Lett.*, vol. 121, no. 20, p. 201801, 2018.
- [4] J. L. Miller, “Accelerator experiments are closing in on neutrino CP violation,” *Phys. Today*, vol. 73, no. 6, pp. 14–16, 2020.
- [5] K. Abe *et al.*, “Constraint on the matter–antimatter symmetry-violating phase in neutrino oscillations,” *Nature*, vol. 580, no. 7803, pp. 339–344, 2020. [Erratum: *Nature* 583, E16 (2020)].
- [6] Y. Fukuda *et al.*, “Evidence for oscillation of atmospheric neutrinos,” *Phys. Rev. Lett.*, vol. 81, pp. 1562–1567, 1998.
- [7] Q. R. Ahmad *et al.*, “Direct evidence for neutrino flavor transformation from neutral current interactions in the Sudbury Neutrino Observatory,” *Phys. Rev. Lett.*, vol. 89, p. 011301, 2002.
- [8] M. C. Gonzalez-Garcia, M. Maltoni, and T. Schwetz, “NuFIT: Three-Flavour Global Analyses of Neutrino Oscillation Experiments,” *Universe*, vol. 7, no. 12, p. 459, 2021.
- [9] Alam *et al.*, “Completed sdss-iv extended baryon oscillation spectroscopic survey: Cosmological implications from two decades of spectroscopic surveys at the apache point observatory,” *Phys. Rev. D*, vol. 103, p. 083533, Apr 2021.

- [10] N. Aghanim *et al.*, “Planck 2018 results. VI. Cosmological parameters,” *Astron. Astrophys.*, vol. 641, p. A6, 2020. [Erratum: *Astron. Astrophys.* 652, C4 (2021)].
- [11] M. Agostini *et al.*, “Final Results of GERDA on the Search for Neutrinoless Double- β Decay,” *Phys. Rev. Lett.*, vol. 125, no. 25, p. 252502, 2020.
- [12] D. Q. Adams *et al.*, “Improved Limit on Neutrinoless Double-Beta Decay in ^{130}Te with CUORE,” *Phys. Rev. Lett.*, vol. 124, no. 12, p. 122501, 2020.
- [13] M. Aker *et al.*, “Direct neutrino-mass measurement with sub-electronvolt sensitivity,” *Nature Phys.*, vol. 18, no. 2, pp. 160–166, 2022.
- [14] S. Dimopoulos, S. Raby, and F. Wilczek, “Supersymmetry and the Scale of Unification,” *Phys. Rev. D*, vol. 24, pp. 1681–1683, 1981.
- [15] N. Haba and T. Ota, “Vanishing dimension five proton decay operators in the SU(5) SUSY GUT,” *Acta Phys. Polon. B*, vol. 39, pp. 1901–1912, 2008.
- [16] S. Heinemeyer, Mondragon, *et al.*, “The Higgs boson discovery: recent implications for the Finite Unified Theories and SUSY breaking scale,” *PoS*, vol. CORFU2017, p. 081, 2018.
- [17] Y. Yamada, “SUSY and GUT threshold effects in SUSY SU(5) models,” *Z. Phys. C*, vol. 60, pp. 83–94, 1993.
- [18] N. N. Singh and S. B. Singh, “Third generation Yukawa couplings unification in supersymmetric SO(10) model,” *Eur. Phys. J. C*, vol. 5, pp. 363–367, 1998.
- [19] K. S. Singh and N. N. Singh, “Effects of the Variation of SUSY Breaking Scale on Yukawa and Gauge Couplings Unification,” *Adv. High Energy Phys.*, vol. 2015, p. 652029, 2015.
- [20] S. Dawson, “Introduction to Electroweak Symmetry Breaking,” *AIP Conf. Proc.*, vol. 1116, no. 1, pp. 11–34, 2009.

- [21] S. Dawson, “The MSSM and why it works,” *Theoretical Advanced Study Institute in Elementary Particle Physics , TASI’97. Proc.*, pp. 261–339, 1997.
- [22] R. Goncalo, S. Guindon, and V. Jain, “Sensitivity of LHC experiments to the $t\bar{t}H$ final state, with $H \rightarrow b\bar{b}$, at center of mass energy of 14 TeV,” *Contribution to Community Summer Study 2013 on the Future of U.S. Particle Physics: Snowmass on the Mississippi , CSS2013.*, p. 4, 2013.
- [23] A. K. Chaudhuri, “Large elliptic flow in low multiplicity pp collisions at LHC energy $s^{*(1/2)} = 14\text{-TeV}$,” *Phys. Lett. B*, vol. 692, pp. 15–19, 2010.
- [24] L. Randall and M. Reece, “Single-Scale Natural SUSY,” *JHEP*, vol. 08, p. 088, 2013.
- [25] K. Yonekura, “Single scale model of SUSY breaking, gauge mediation, and dark matter,” *Soryushiron Kenkyu Electron.*, vol. 119, p. 1, 2011.
- [26] R. L. Arnowitt and P. Nath, “SUSY mass spectrum in SU(5) supergravity grand unification,” *Phys. Rev. Lett.*, vol. 69, pp. 725–728, 1992.
- [27] Y. Yamada, “SUSY and GUT threshold effects in SUSY SU(5) models,” *Z. Phys. C*, vol. 60, pp. 83–94, 1993.
- [28] S. Antusch, J. Kersten, M. Lindner, and M. Ratz, “Running neutrino masses, mixings and CP phases: Analytical results and phenomenological consequences,” *Nucl. Phys. B*, vol. 674, pp. 401–433, 2003.
- [29] D. R. T. Jones and L. Mezincescu, “The Beta Function in Supersymmetric Yang-Mills Theory,” *Phys. Lett. B*, vol. 136, pp. 242–244, 1984.
- [30] K. S. Singh, S. Roy, and N. N. Singh, “Stability of neutrino parameters and self-complementarity relation with varying SUSY breaking scale,” *Phys. Rev. D*, vol. 97, no. 5, p. 055038, 2018.
- [31] V. D. Barger, M. S. Berger, and P. Ohmann, “Supersymmetric grand unified theories: Two loop evolution of gauge and Yukawa couplings,” *Phys. Rev. D*, vol. 47, pp. 1093–1113, 1993.
- [32] P. Zyla *et al.*, “Review of Particle Physics,” *PTEP*, vol. 2020, no. 8, p. 2093, 2020. and 2021 update.

- [33] J. E. Bjorkman and D. R. T. Jones, “The Unification Mass, $\text{Sin}^2\theta_W$ and M_b/M_τ in Nonminimal Supersymmetric SU(5),” *Nucl. Phys. B*, vol. 259, p. 533, 1985.
- [34] M. Patgiri and N. N. Singh, “New uncertainties in QCD-QED rescaling factors using quadrature method,” *Pramana*, vol. 65, pp. 1015–1025, 2006.
- [35] Y. Kajiyama, M. Raidal, and A. Strumia, “The Golden ratio prediction for the solar neutrino mixing,” *Phys. Rev. D*, vol. 76, p. 117301, 2007.
- [36] L. L. Everett and A. J. Stuart, “Icosahedral (A(5)) Family Symmetry and the Golden Ratio Prediction for Solar Neutrino Mixing,” *Phys. Rev. D*, vol. 79, p. 085005, 2009.
- [37] A. Sirunyan, A. Tumasyan, and other, “A measurement of the higgs boson mass in the diphoton decay channel,” *Physics Letters B*, vol. 805, p. 135425, 2020.